HARDWARE-DRIVEN COMPRESSIVE SAMPLING FOR FAST TARGET LOCALIZATION USING SINGLE-CHIP UWB RADAR SENSOR

Sungwon Lee, Chenliang Du , Hossein Hashemi and Antonio Ortega

Ming Hsieh Department of Electrical Engineering
University of Southern California
sungwonl@usc.edu, chenliad@usc.edu, hosseinh@usc.edu, ortega@sipi.usc.edu

ABSTRACT

To design an energy-efficient UWB ranging system, we propose a compressive sampling (CS) technique tightly coupled to a recently proposed hardware. Our goal is to design a system that is robust to high noise and consumes less energy while providing reliable localization. In this work, we first introduce a representation of UWB signals as group sparse signals with the number of groups corresponding to the number of objects in the environment. Also, we design an efficient measurement system that is constructed using low-density parity-check (LDPC) matrix, in order to satisfy several constraints imposed by the hardware: non-negative integer entries in measurement (sensing) matrix, constant row-wise sum of non-zero entries in the matrix, and a unique structure characterized by Kronecker product. To enhance performance, we propose a window-based reweighted L_1 minimization that outperforms other existing algorithms in our simulation. The result shows that our proposed method can achieve reliable target-localization, while using only 40% of the scanning (sampling) time required by the sequential scanning scheme, even in highly-noisy environments.

Index Terms— compressive sampling (CS), ultra wideband radar, low-density parity check code, target localization

1. INTRODUCTION

Ultra-wideband (UWB) systems have been utilized for important applications such as UWB radar tracking objects in space and monitoring breathing or heartbeats of humans [1, 2]. For example, breathing monitoring can be achieved by localizing the subject's chest movement, which is critical for people who are under severe injury or sedation after surgery. This requires a precise and fast localization of objects with high resolution. Compared to available solutions using video camera techniques, UWB provides benefits of higher spatial depth resolution [3].

In general, UWB radar sensors employ two types of detection schemes: (i) energy detection [4] or (ii) direct sampling [5, 6]. Energy detection achieves low power consumption and has a simple architecture due to the nature of correlator-based detection circuitry. At the expense of higher power consumption, direct sampling enables the reconstruction of the reflection waveform in the whole detection range and therefore provides opportunity for advanced signal processing to extract additional information [7]. A practical challenge for UWB radar design is to overcome the low SNR from each received pulse due to the UWB emission spectrum mask posed by Federal Communications Commission (FCC) [8].

A recently developed hardware [5, 6] adopts direct sampling approach, utilizing a *ranging* technique by sending multiple pulses then averaging the received pulses in short time intervals (*windows*), each corresponding to a certain roundtrip time of the reflected pulse. Assuming the environment is relatively static, the receiver can localize an object at a specific distance by selecting a corresponding window and determining if the window contains reflected signal. The averaging within a chosen window provides robustness to noise. It also requires less power consumption, because power is only consumed during the measurement window, which can represent a small percentage of time. However, a limitation of this scheme comes from sequential sampling, i.e., candidate object locations have to be probed in sequence, so that the time required to locate an object will be proportional to the number of measurement windows. In this paper we propose techniques that can significantly reduce the scanning time, with no increase in overall power consumption. The key observation is that in many situations the number of objects that can be observed is small relative to the number of locations that are probed. This allows us to probe several locations simultaneously, so that each measurement combines reflections at several distances. The processing can be used extract the actual position information from the combined observations. Our approach is based on compressed sensing (CS) principles with a design that tightly coupled to the UWB hardware platform.

In the context of radar applications, many researchers have proposed CS-based approaches thanks to the sparse structure of UWB signal [9, 10]. In [11], authors showed that the received signal can be digitized at a rate much lower than the Nyquist rate, without a need for matched filters. But, they ignore some important issues, such as the high noise case and total power consumption. Similarly, CS was applied to UWB detection applications, but with a mostly theoretical focus [12–14] or with experiments in a relatively simple environment [15]. Also, a precise CS-UWB positioning system was proposed by exploiting the redundancy of UWB signal captured at multiple receivers to localize a transmitter [16, 17]. This work achieved low ADC sampling rate but the rate is higher than that of our UWB hardware platform also does not show robustness to large amount of noise. As a CS approach tightly coupled to hardware, Random-Modulation Pre-Integrator (RMPI) was proposed to achieve low-rate ADC by random modulation in analog domain [18–20] but their hardware appropriate to low-rate signal acquisition imposes different constraints, i.e. block-diagonal sensing matrix with Bernoulli random entries, from those by our UWB hardware.

In this work, we propose a CS technique tightly coupled to capabilities of recently developed hardware [5, 6] in order to design a system that is robust to high noise and consumes less power while providing reliable localization. First, we formulate sparse structure of signal of interest. The UWB signal is sparse due to two main sources: temporal localization of pulses and existence of few objects. Combined with the UWB ranging system, this leads to a special structure where sparse non-zero entries are clustered into a few groups (windows). The number of groups is equal to the number of object in the region of interest. Second, we design an efficient measurement system subject to several constraints imposed by the hardware. The constraints include (i) non-negative integer entries in sensing matrix (ii) constant row-wise sum of entries in the matrix (iii) unique structure characterized by a Kronecker product. Under the constraints, we construct a sensing matrix by using low-density parity-check (LDPC) matrix which is recently shown as a good measurement system in [21, 22]. Third, to enhance the localization performance, we propose a window-based reweighted L_1 minimization which shows good performance for abovementioned signal model and measurement system. In simulation, we compare our proposed method with other existing reconstruction algorithms with respect to several metrics evaluating localization performance. Our simulation result shows that our proposed method can achieve reliable target-localization while using only 40% of the sampling time required by the corresponding sequential scanning scheme, even in a highly-noisy environment.

2. PROBLEM FORMULATION

2.1. UWB Ranging System

A recently proposed hardware design [5, 6] provides a receiver that can probe for the presence of objects within a small range of distances. This is illustrated in Fig. 1. In this approach, short-time pulses are transmitted periodically and we determine a short time interval (window) which contains the reflected signal. Under the assumption that the reflected signal resides within a window without overlapping with the others, we can localize an object in a distance from the receiver by identifying the window. Denoting cycle the interval between successive transmitted pulses as shown in Fig. 1, we divide a cycle into windows, each corresponding to a small distance range.

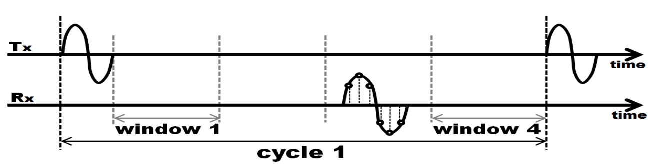

Fig. 1. Basic motivation for UWB ranging system. The short-time pulses are transmitted periodically over multiple cycles and the rangin system determines a short time interval (window) which contains the reflected signal.

The hardware design has several advantages: low power consumption, robustness to large amount of noise, and freedom to choose different sampling algorithms. By selecting a specific range, the system cannot observe objects at other distances, because measurements are performed only within the chosen window. But, as a consequence, power consumption is significantly reduced, since no power is consumed during other window intervals, while averaging over multiple cycles provides robustness to noise. Also, the averaging makes the hardware design robust to large amounts of noise at the receiver, e.g. thermal noise from circuits, reflection from objects that are not of interest, etc. The power of noise is significantly high compared with the original signal to reconstruct; the upper bound of SNR with the hardware design is about -21dB based on the discussion in [23]. Furthermore, the system does not consume extra energy when changing windows to sample, thus this gives freedom to develop better sampling algorithm by measuring signals in multiple windows which motivates our new sampling scheme.

2.2. Sparse UWB Signal Model based on Windows

Without noise, e.g. thermal noise from circuits and multipath reflections from objects out of interest, the sampled signal, $\boldsymbol{x}$, will be sparse because of two main reasons. First, UWB pulses are very narrow in time, so that the received signals are themselves sparse in the time domain, i.e., reflected pulses corresponding to an object of interest are present in a short time interval. Second, the number of objects of interest is small compared to the number of windows. Thus, $\boldsymbol{x}$ has a special structure such that sparse non-zero entries are clustered within a few windows, with the number of windows equals to the number of objects in the region of interest.

Let N_s be the number of samples in each window, and assume that the UWB-ranging system has non-overlapped N_w windows in each cycle, each of which can capture all reflections from a specific distance from the receiver. Thus, $\boldsymbol{x}$ can be divided into N_W sub-signals, $\boldsymbol{x}^i, i \in 1, ..., N_w$:

$$\boldsymbol{x}^T = [\underbrace{x_1, \ldots, x_{N_S}}_{\boldsymbol{x}^1}, \ldots, \underbrace{x_{N-N_S+1}, \ldots, x_N}_{\boldsymbol{x}^{N_w}}]^T \tag{1}$$

Since every $\boldsymbol{x}^i$ has a length of N_S, the dimension of $\boldsymbol{x}$, N, is $N_s N_w$. Our signal model based on windows is similar to those proposed by other researchers such as block-sparsity, cluster-sparsity, or multiple measurement vector (MMV) model [24–26]. Our sparse signal, $\boldsymbol{x}$, is a simplified version of them with non-overlapped and equal-sized groups of non-zero entries. However, this signal model, to the best of our knowledge, have not been applied to UWB signal measured by a realistic hardware with ranging capability.

2.3. UWB Measurement System and Matrix Formulation

Consider the system in [5,6] and let N_c be the number of cycles over which the receiver integrates before the ADC is activated. After the integrated analog waveform is sampled by the ADC, the receiver obtains $N(= N_s N_w)$ samples in total. Since we take a summation of samples to collect measurements, $\boldsymbol{y}$, we can represent $\boldsymbol{y}$ as linear combinations of $\boldsymbol{x}$. Thus, a sampling scheme can be expressed as $\boldsymbol{y} = \boldsymbol{\Phi}\boldsymbol{x} + \boldsymbol{n}$ with sensing matrix, $\boldsymbol{\Phi}$ and noise vector, $\boldsymbol{n}$. Here, $\boldsymbol{n}$ is a vector of the same length of $\boldsymbol{y}$ and each entry, $\boldsymbol{n}(i)$, is a summation of random variables following i.i.d. Gaussian distribution, $N(0, \sigma_N^2)$: $\boldsymbol{n}(i) = \Sigma_{i=1}^{N_c} n_i, n_i \sim N(0, \sigma_N^2)$.

Since the UWB ranging hardware obtains measurements based on windows, we can formulate $\boldsymbol{\Phi}$ as a matrix containing blocks with the dimension of N_s-by-N_s, each corresponding to a specific window. Also, $\boldsymbol{\Phi}$ contains non-negative integer entries indicating the number of cycles integrated in order to obtain measurements. In details, $\Phi(i,j)$ indicates the number of cycles for $x(j)$ to be integrated to obtain $y(i)$. Thus, we can easily compute the total scanning time by taking summation of all the (non-zero) entries in $\boldsymbol{\Phi}$: $\sum_{\forall i,j} \boldsymbol{\Phi}(i,j)$.

In this work, we consider two sampling schemes: (i) sequential sampling scheme presented in [5, 6] and (ii) hardware-driven compressive sampling (HDCS) proposed in this paper. As shown in Fig. 2, the sequential sampling scheme scans each *identical* window over 5 cycles, $N_c = 5$, until it scans all 4 windows, $N_w = 4$. Thus, each measurement, $y(i)$, is obtained by taking summation of $x(i)$ five times with additional noise. On the contrary, HDCS scheme collects information about *multiple* windows from a measurement by

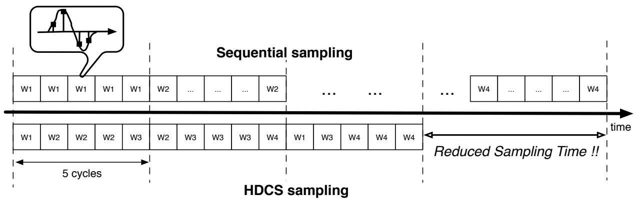

Fig. 2. Advantage of HDCS scheme. The measurements are obtained from 4 windows containing 4 samples throughout 5 cycles: $N_s = 4$, $N_w = 4$, and $N_c = 5$. While Sequential sampling scans a single window during 5 cycles, HDCS collects information from multiple windows during 5 cycles, which leads to sampling time reduction.

scanning a certain combinations of windows within 5 cycles. Here, we fix the number of cycles for windows to be scanned for a measurement as $N_c = 5$ for simplicity, thus we can achieve faster scanning by reducing the number of measurements.

These sampling processes can be represented by a matrix formulation. The sequential sampling scheme in Fig. 2 can be represented by a *diagonal* sensing matrix with the N_c on its diagonal as $\mathbf{\Phi_1}$ in Eq. (2).

$$\mathbf{\Phi_1} = \begin{bmatrix} 5\boldsymbol{I} & \mathbf{0} & \mathbf{0} & \mathbf{0} \\ \mathbf{0} & 5\boldsymbol{I} & \mathbf{0} & \mathbf{0} \\ \mathbf{0} & \mathbf{0} & 5\boldsymbol{I} & \mathbf{0} \\ \mathbf{0} & \mathbf{0} & \mathbf{0} & 5\boldsymbol{I} \end{bmatrix}_{16\times 16}, \quad \mathbf{\Phi_2} = \begin{bmatrix} 1\boldsymbol{I} & 3\boldsymbol{I} & 1\boldsymbol{I} & \mathbf{0} \\ \mathbf{0} & 1\boldsymbol{I} & 3\boldsymbol{I} & 1\boldsymbol{I} \\ 1\boldsymbol{I} & \mathbf{0} & 1\boldsymbol{I} & 3\boldsymbol{I} \end{bmatrix}_{12\times 16} \tag{2}$$

However, HDCS sensing matrix, $\mathbf{\Phi_2}$, does not necessarily have non-zero entries on its diagonal depending on the combinations of widows providing information for measurements. The intuition of HDSC is similar to one in our previous work [27] such that energy-efficient data gathering can be achieved by collecting measurements from multiple clusters on wireless sensor network. If $\mathbf{\Phi_2}$ can give us the same level of reconstruction as $\mathbf{\Phi_1}$, we can achieve 0.75 scanning time reduction which leads to the same amount of total power consumption as shown in Fig. 2. Now, the challenge is how to design a *good* sensing matrix satisfying the constrains imposed by the hardware.

3. PROPOSED APPROACH

3.1. LDPC Measurement System

In order to reduce the scanning time, the challenges are how to design a measurement mechanism that can achieve successful reconstruction with fewer measurements. With traditional CS, the underdetermined sensing matrices such as Gaussian random matrix and (uniform randomly) down-sampled Fourier matrix have been exploited as sensing matrices because they satisfy Restricted Isometry Property (RIP) with high probability [10].

However, combined with UWB ranging system [5,6], these popular sensing matrices are no longer appropriate due to three additional constraints: i) all the entries of the matrix should be non-negative integers because the entries indicate the number of cycles. This condition rules out popular sensing matrices such as random or Fourier matrices that have real entries. ii) the sum of entries in each row is fixed as a constant number of cycles, N_c, for simplicity. Thus, the scanning time is directly proportional to the number of rows in the sensing matrix. iii) non-zero entries of each row can exist only at the positions with constant shift of N_s. Thus, sensing matrix, $\mathbf{\Phi}$, can be formulated as a Kronecker product of the identity matrix with a matrix containing coefficients at the corresponding positions, $\boldsymbol{A}$ (effective sensing matrix):

$$\mathbf{\Phi}_{M\times N} = \begin{bmatrix} a_{(1,1)}\boldsymbol{I} & \dots & a_{(1,N_W)}\boldsymbol{I} \\ \vdots & \ddots & \vdots \\ a_{(M_W,1)}\boldsymbol{I} & \dots & a_{(M_W,N_W)}\boldsymbol{I} \end{bmatrix} = \boldsymbol{A}_{M_W\times N_W} \otimes \boldsymbol{I}_{N_S} \tag{3}$$

To satisfy the conditions imposed by the hardware, we propose to adopt low-density parity-check (LDPC) measurement system recently studied in [21, 22]. In [21], authors provide strong theoretical results showing that parity-check matrices of good channel codes can be used as provably good measurement matrices under basis pursuit. In [22], authors show that LDPC matrices significantly outperform other current CS matrices. Thus, by using LDPC matrix as the effective sensing matrix, $\boldsymbol{A}$, we can construct a good sensing matrix, $\mathbf{\Phi}$ by Eq. (3) because the coherence of sensing matrix, $\mathbf{\Phi}$, is the same as effective sensing matrix, $\boldsymbol{A}$. This can be easily shown as $\boldsymbol{U_\Phi} = \mathbf{\Phi^T \Phi} = (\boldsymbol{A} \otimes \boldsymbol{I})^T (\boldsymbol{A} \otimes \boldsymbol{I}) = \boldsymbol{A^T A} \otimes \boldsymbol{I} = \boldsymbol{U_A} \otimes \boldsymbol{I}$. Thus, if $\boldsymbol{A}$ is a good CS measurement matrix, then $\mathbf{\Phi}$ in Eq. (3) is also a good sensing matrix. Also, since LDPC matrices have the same number of 1's in each row, we can construct $\mathbf{\Phi}$ by evenly distributing N_c cycles over the non-zero entries of LDPC matrix, which satisfies the second condition.

3.2. Window-based Reweighted L_1 Minimization

In reconstruction, the goal is to identify the data support which contains the non-zero entries because the data support uniquely corresponds to the locations in space. With sequential sampling scheme in [5, 6], we can reconstruct a signal, $\hat{\boldsymbol{x}}$, by dividing integrated measurements by the number of cycles, N_c. Then, thresholding is applied with a empirically chosen threshold in order to determine data support. With this technique, more cycles provide higher SNR because the noise can be approximated as identically independent Gaussian noise. However, the approach requires large number of cycles enough to remove the noise. Also, this should scan all the windows sequentially so that it results in longer scanning time (or higher power consumption).

With HDCS scheme discussed in Section 3.1, we propose two-phase localization: non-linear signal reconstruction and thresholding. For successful reconstruction of the signal with powerful noise, we propose iterative window-based reweighted L_1 minimization (WRL_1). In details, we iteratively minimize L_1 norm of weighted sum of intermediate $\boldsymbol{x_i}$ subject to data-fitting constraint: $\min \| \sum_{\forall j,k} \boldsymbol{W_i^j}(k) \boldsymbol{x_i^j}(k) \|_1$ s.t. $\|\mathbf{\Phi} \boldsymbol{x_i} - \boldsymbol{y}\|_2 \leq \delta$. Here, we adopt a classical trick that has been used in iterative reweighted L_1 minimization but the only difference is that the weight is computed by window-wise operation. the weight vector of the j^{th} window at the i^{th} iteration, $\boldsymbol{W}_i[j]$, is

$$\boldsymbol{W_i^j} = \mathbf{1} \frac{1}{\|\boldsymbol{x}_{i-1}^j\|_1 + \epsilon}, \; j \in \{1, \dots, N_W\}, \tag{4}$$

where $\mathbf{1}$ is a vector with the value of 1 and the dimension of N_S. The weights for the entries belonging to k^{th} window are computed as L_1 norm of partial intermediate signal, $\boldsymbol{x}[k]$, within that window. Thus, the weight increases as the energy in the corresponding becomes smaller, which indicates that this algorithm provides equal chance to find the right solution over all the windows. The updating scheme based on windows is similar to the adaptive group lasso algorithm [28] or reweighted M-Basis Pursuit in [26]. For thresholding, a window is chosen as one of the possible data supports if the energy of the window is greater than a empirically chosen threshold, $\|\hat{\boldsymbol{x}}[k]\|_2 > 0.001$. Note that the threshold is fixed throughout this paper, not changing according to different noise levels or different number of measurements.

4. SIMULATION RESULT

For simulation, we consider 155 windows which contains 16 samples thus the signal of interest, $\boldsymbol{x}$, has a length of $N = N_w N_s = 2480$. Also we assume that we obtain one measurement through 500 cycles: $N_c = 500$. In the simulation, the goal is to localize three objects in the region of interest. We generated a data set of 80 realizations and each data contains three windows with non-zero entries indicating three objects in space; those windows are chosen with uniformly random manner and the values of non-zero entries are generated by Gaussian distribution.

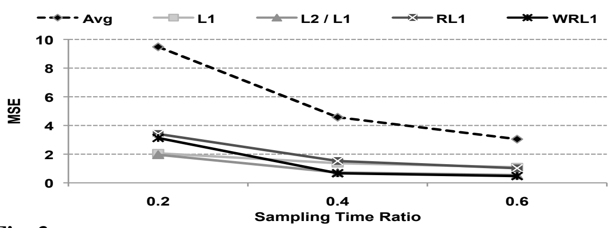

Fig. 3. Cost ratio vs. MSE: For CS sampling schemes, cost is the total sampling time to collect M measurements. Since we fix the number of cycles, N_c, for every measurement as 500 in the simulation, the cost ratio is a ratio of the number of measurements to the dimension of signal, M/N. But, for sequential sampling scheme (noted 'Avg' in the figure), we take N measurements with reduced N_c.

As discussed in Section 3.1, we construct measurement matrix using LDPC matrices with different number rows, M_w, by changing the number of 1's in each column from 1 to 3 with that in each row fixed as 5. Then, 500 (cycles) are evenly distributed over non-zero entries (1's) in each row thus $\boldsymbol{A}$ has 5 non-zero entries with the value of 100 in each row. Also, we consider noisy measurements with three different noise levels, $\sigma_N \in \{10, 20, 30\}$, which generates very low SNR (approximately -16.5dB, -22.6dB and -26.1dB on average over our data set, respectively). For reconstruction, we compare window-based reweighted L_1 minimization (WRL_1), with three other algorithms: traditional L_1 minimization (L_1) [9, 10], L_2/L_1 minimization (L_2/L_1) [24], and reweighted L_1 minimization (RL_1) [29, 30].

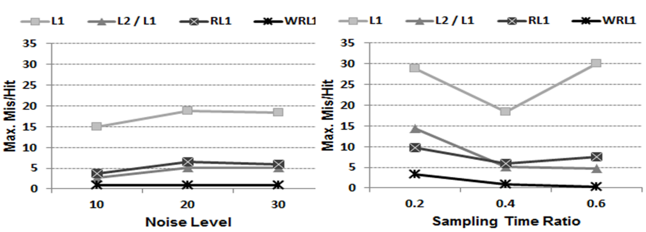

(a) σ_N vs. max. mis-hit (b) sampling time ratio vs. max. mis-hit

Fig. 4. Performance comparison with respect to maximum mis-hit of data support: (a) Fix sampling time ratio as 0.4 and compare performance at different noise levels. (b) Fix noise level as 30 and compare performance at different sampling time ratios.

To evaluate performance, we need to measure localization quality as well as scanning time. The scanning time can be easily computed by counting the number of rows of sensing matrix, $\boldsymbol{\Phi}$, because we fix the number of cycles (N_c) for every measurement as 500 in the simulation. Thus, the cost ratio is a ratio of the number of measurements to the dimension of signal, M/N. To evaluate localization quality, Mean Squared Error (MSE) can be used by measuring the entry-wise difference of values between $\boldsymbol{x}$ and $\hat{\boldsymbol{x}}$. Fig. 3 shows the performance comparison of our proposed reconstruction technique, WRL_1, to other reconstruction techniques with respect to MSE and scanning time. However, for sequential sampling scheme (noted 'Avg' in the figure) [5, 6], we take N measurements with reduced N_c'. To compare two sampling schemes, N_c' is chosen as $\frac{MN_c}{N}$ because $N_c' N_w N = M N_w N_c$. Thus, $N_c' = \frac{N_c M}{N_w N_s} = 0.202M$. The result shows that HDCS schemes with different reconstruction techniques achieve about five times better reconstruction quality with similar scanning time.

Although Mean Squared Error (MSE) is one of the most generic metric for reconstruction evaluation, it can be misleading because smaller MSE does not always guarantee better window identification. For example, perfect identification of data support can result in large MSE if the large difference between $\boldsymbol{x}$ and $\hat{\boldsymbol{x}}$ exists within the correct data support. Thus, we consider two additional metrics to evaluate mismatch of data support: maximum mis hit and F-measure. (i) To evaluate the performance in the worst case, we consider the maximum mis hit of data support by computing the maximum distance (in terms of "window") between chosen windows from the thresholding of $\hat{\boldsymbol{x}}$ and the ground truth. (ii) We also compute F-measure discussed in [26] as $2\frac{|supp(\boldsymbol{x}) \cap supp(\hat{\boldsymbol{x}})|}{|supp(\boldsymbol{x})| + |supp(\hat{\boldsymbol{x}})|}$, where $supp(\boldsymbol{x}) = \{i \in [1, \ldots, N_W] : \|\boldsymbol{x}[i]\|_2 > 0.001\}$. Note that the F-measure is equal to 1 when the data support of the reconstructed signal coincides exactly with the ground truth.

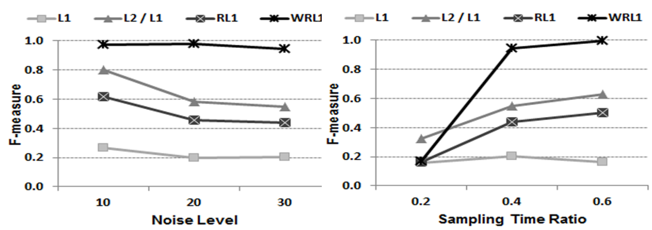

(a) σ_N vs. F-measure (b) sampling time ratio vs. F-measure

Fig. 5. Performance comparison with respect to F-measure: (a) Fix sampling time ratio as 0.4 and compare performance at different noise levels. (b) Fix noise level as 30 and compare performance at different sampling time ratios.

Fig. 4 and Fig. 5 compare performance with respect to above-mentioned two metrics. Here, we do not consider sequential sampling scheme because the scheme requires a empirically chosen threshold for data-support identification and this hurts fair comparison. In Fig. 4(a), WRL_1 shows very small maximum mismatch at every noise level which is almost equal to 1. This indicates that our identified windows are mismatched at most by one window on average over 80 data. Also, WRL_1 shows very stable performance at different noise levels. Fig. 4(b) shows that, in the highest level of noise we tested, WRL_1 shows the best performance and it reaches to almost perfect reconstruction at 0.6 sampling time ratio. Similarly, in Fig. 5(a), WRL_1 shows the highest F-measure at every noise level which is very close to 1. Also, it does not drop as the noise level increases as shown in Fig. 5(b).

5. CONCLUSION

To design energy-efficient UWB ranging system, we propose a CS approach incorporated with a novel hardware structure. we first formulate UWB signal with a special structure that sparse non-zero entries are clustered into a few groups. Also, we design an efficient measurement system that is constructed by low-density parity-check (LDPC) matrix, which satisfies several constraints imposed by the hardware. To enhance performance, we propose a window-based reweighted L_1 minimization which outperforms other existing algorithms in our simulation. The result shows that our proposed method can achieve reliable target-localization only with 40% of sampling time of the sequential sampling scheme in highly-noisy environment.

6. REFERENCES

[1] E. Conti, A. Filippi, and S. Tomasin, "On the modulation of ultra wide band pulse radar signal by target vital signs," *International Symposium on Bioelectronics and Bioinformatics*, Dec. 2009.

[2] S. H. Chang, R. Sharan, M. Wolf, N. Mitsumoto, and J. Burdick, "Uwb radar-based human target tracking," *IEEE Radar Conference*, May 2009.

[3] C. Li, J. Ling, J. Li, and J. Lin, "Accurate doppler radar noncontact vital sign detection using the relax algorithm," *IEEE Transactions on Instrumentation and Measurement*, vol. 59, no. 3, pp. 687–695, 2010.

[4] H. Krishnaswamy and H. Hashemi, "A 4-channel 4-beam 24-to-26GHz spatio-temporal RAKE radar transceiver in 90nm CMOS for vehicular radar applications," *IEEE International Solid-State Circuits Conference Digest of Technical Papers*, pp. 214–215, 2010.

[5] T. Chu, J. Roderick, S. Chang, T. Mercer, C. Du, and H. Hashemi, "A short-range uwb ir cmos sensor for human feature detection," *IEEE International Solid-State Circuits Conference Digest of Technical Papers*, pp. 294–295, Feb. 2011.

[6] C. Du and H. Hashemi, "An uwb cmos impulse radar," *to be appeared in IEEE Radio Frequency Integrated Circuits Symposium*, 2013.

[7] S. Chang, M. Wolf, and J. W. Burdick, "Human detection and tracking via ultra-wideband (UWB) radar," *IEEE International Conference on Robotics and Automation*, May 2010.

[8] Federal Communications Commission, "First report and order, revision of part 15 of the commission's rules regarding ultra wideband transmission systems," *ET Docket*, pp. 98–153, Feb 2002.

[9] E.J. Candès, J.K. Romberg, and T. Tao, "Stable signal recovery from incomplete and inaccurate measurements," *Communications on Pure and Applied Mathematics*, vol. 59, no. 8, pp. 1207, 2006.

[10] D. L. Donoho, "Compressed sensing," *IEEE Transactions on Information Theory*, Apr. 2006.

[11] R. Baraniuk and P. Steeghs, "Compressive radar imaging," *IEEE Radar Conf*, pp. 128–133, 2007.

[12] M. Herman and T. Strohmer, "High resolution radar via compressed sensing," *preprint*, 2007.

[13] F.M. Naini, R. Gribonval, L. Jacques, and P. Vandergheynst, "Compressive sampling of pulse trains: Spread the spectrum!," *International Conference on Acoustics, Speech, and Signal Processing (ICASSP)*, 2009.

[14] JL Paredes, GR Arce, and Z. Wang, "Ultra-wideband compressed sensing: Channel estimation!," *IEEE Journal of Selected Topics in Signal Processing*, vol. 1, no. 3, pp. 383–395, 2007.

[15] G. Shi, J. Lin, X. Chen, F. Qi, D. Liu, and L. Zhang, "Uwb echo signal detection with ultra-low rate sampling based on compressed sensing," *IEEE Transactions on Circuits and Systems II: Express Briefs*, vol. 55, no. 4, pp. 379–383, 2008.

[16] D. Yang, H. Li, G. D. Peterson, and A. Fathy, "UWB signal acquisition in positioning systems: Bayesian compressed sensing with redundancy," *Conference on Information Sciences and Systems (CISS)*, 2009.

[17] D. Yang, Husheng Li, and G.D. Peterson, "Compressed sensing tdoa for UWB positioning systems," *IEEE Radio and Wireless Symposium (RWS)*, 2011.

[18] J. Yoo, C. Turnes, E. Nakamura, C. Le, S. Becker, E. Sovero, M. Wakin, M. Grant, J. Romberg, A. Emami-Neyestanak, and E. Candès, "A compressed sensing parameter extraction platform for radar pulse signal acquisition," *IEEE Journal on Emerging and Selected Topics in Circuits and Systems (JETCAS)*, vol. PP, no. 99, pp. 1–13, 2012.

[19] M. Loh M. Monge E. Candès A. Emami-Neyestanak J. Yoo, S. Becker, "Design and implementation of a fully integrated compressed-sensing signal acquisition system," *IEEE International Conference on Acoustics, Speech, and Signal Processing (ICASSP)*, 2012.

[20] M. Loh M. Monge E. Candès A. Emami-Neyestanak J. Yoo, S. Becker, "A 100mhz-2ghz 12.5x sub-nyquist rate receiver in 90nm cmos," *IEEE Radio Frequency Integrated Circuits Symposium (RFIC)*, 2012.

[21] A. G. Dimakis, R. Smarandache, and P. O. Vontobel, "Ldpc codes for compressed sensing," *To appear, IEEE Transactions on Information Theory*, 2012.

[22] W. Lu, K. Kpalma, and J. Ronsin, "Sparse binary matrices of ldpc codes for compressed sensing," *Data Compression Conference (DCC)*, 2012.

[23] Kraus, "Antennas," in *McGraw-Hill*, 1988, pp. 774–790.

[24] Y. Eldar and M. Mishali, "Robust recovery of signals from a union of subspaces," *preprint*, 2008.

[25] R.G. Baraniuk, V. Cevher, M. Duarte, and C. Hegde, "Model-based compressive sensing," *IEEE Transactions on Information Theory*, vol. 56, no. 4, pp. 1982–2001, 2010.

[26] A. Rakotomamonjy, "Surveying and comparing simultaneous sparse approximation (or group-lasso) algorithms," *Signal Processing*, vol. 91, pp. 1505–1526, 2011.

[27] S. Lee and A. Ortega, "Joint optimization of transport cost and reconstruction for spatially- localized compressed sensing in multi-hop sensor networks," *APSIPA*, Dec. 2010.

[28] H. Zou, "The adaptive lasso and its oracle properties," *Journal of the American Statistical Association*, vol. 101, no. 476, pp. 1418–1429, 2006.

[29] E. J. Candès, M. B. Wakin, and S. Boyd, "Enhancing sparsity by reweighted l1 minimization," *Journal of Fourier Analysis and Applications,*, vol. 14, no. 5, pp. 877–905, Dec. 2008.

[30] R.Saab, R.Chartrand, and Ozgur Yilmaz, "Stable sparse approximations via nonconvex optimization," *International Conference on Acoustics, Speech, and Signal Processing (ICASSP)*, 2008.